Scaling of spectral anisotropy with magnetic field strength in decaying magnetohydrodynamic turbulence

Sean Oughton, William H. Matthaeus, and Sanjoy Ghosh

Citation: Physics of Plasmas (1994-present) **5**, 4235 (1998); doi: 10.1063/1.873159
View online: http://dx.doi.org/10.1063/1.873159
View Table of Contents: http://scitation.aip.org/content/aip/journal/pop/5/12?ver=pdfcov
Published by the AIP Publishing

Scaling of spectral anisotropy with magnetic field strength in decaying magnetohydrodynamic turbulence

Sean Oughton[a)]
Department of Mathematics, University College London, London WC1E 6BT, United Kingdom

William H. Matthaeus
Bartol Research Institute, University of Delaware, Newark, Delaware 19716

Sanjoy Ghosh[b)]
Space Applications Corp., 901 Follin Lane, Suite 400, Vienna, Virginia 22180

(Received 29 December 1997; accepted 8 September 1998)

Space plasma measurements, laboratory experiments, and simulations have shown that magnetohydrodynamic (MHD) turbulence exhibits a dynamical tendency towards spectral anisotropy given a sufficiently strong background magnetic field. Here the undriven decaying initial-value problem for homogeneous MHD turbulence is examined with the purpose of characterizing the variation of spectral anisotropy of the turbulent fluctuations with magnetic field strength. Numerical results for both incompressible and compressible MHD are presented. A simple model for the scaling of this spectral anisotropy as a function of the fluctuating magnetic field over total magnetic field is offered. The arguments are based on ideas from reduced MHD (RMHD) dynamics and resonant driving of certain non-RMHD modes. The results suggest physical bases for explaining variations of the anisotropy with compressibility, Reynolds numbers, and spectral width of the (isotropic) initial conditions. © *1998 American Institute of Physics.* [S1070-664X(98)02912-7]

I. BACKGROUND

Several lines of investigation have shown that spectral anisotropy is dynamically generated in magnetohydrodynamic (MHD) turbulence when a mean magnetic field ($\mathbf{B}_0$) of sufficient strength is present. For example, experiments with fusion-related machines[1,2] found that correlation lengths computed parallel to $\mathbf{B}_0$ were typically ten times larger than those computed perpendicular to the mean field. In the solar wind, data analysis of MHD-scale fluctuations reveals that the magnetic autocorrelation tensor has a two-component structure,[3,4] suggesting the presence of both a parallel ''slab'' component and a perpendicular ''two-dimensional'' component, and again indicating spectral anisotropy.

On the theoretical side, efforts to explain this type of behavior have often employed the reduced MHD (RMHD) description,[5–7] which in effect assumes anisotropy from the outset[8] while relying on dynamical theory and physical arguments for its justification.[9] In a similar vein, perturbation theory has provided insights into the processes which generate the anisotropy.[10–13]

There is also considerable numerical support. This includes results from both forced and unforced two-dimensional (2D) simulations,[11,14–16] and unforced incompressible and compressible 3D simulations.[17,18] Moreover, while dissipation appears to be essential for the long-time persistence of the anisotropies,[11,17] the precise nature of the dissipation appears not to be crucial.[19] Shell-model closure calculations also evince a similar development of anisotropy.[20]

For incompressible flows, a perturbation theory approach (''weak turbulence'') yields a useful physical explanation for the dynamical development of the anisotropy, in either two or three dimensions.[10,11] The argument is briefly summarized here. Assume that the zeroth-order state consists of linear Fourier modes; these correspond to (propagating) Alfvén waves—provided the Fourier wavevector, $\mathbf{k}$, is not perpendicular to $\mathbf{B}_0$. Suppose two modes interact (nonlinearly) to drive a third, initially unexcited, mode. In order for this resonant triad interaction to occur, at least one of the modes must have its wavevector perpendicular to $\mathbf{B}_0$ (a ''nonpropagating'' or ''zero frequency'' mode, or in the language of turbulence rather than wave theory, a 2D component of the turbulence). As a consequence, the newly excited mode can have a larger $k_\perp$ than either of the driving modes, but not a larger $k_\parallel$. Energy is thus preferentially transferred to modes with $\mathbf{k}$ quasi-perpendicular to $\mathbf{B}_0$, thereby engendering the observed spectral anisotropy.

Note that there has been some recent discussion on the relevance of these resonant triad arguments,[21–24] due to confusion over the nature of Fourier modes with $\mathbf{k}\cdot\mathbf{B}_0=0$. It appears that formulations such as Ref. 21, which take into account only propagating eigenmodes, are only relevant in the case where there is no 2D component to the fluctuations, i.e., when *all* modes with $\mathbf{k}\cdot\mathbf{B}_0=0$ remain unexcited for *all* time.[22–24] This is a rather restrictive condition and is not expected to hold in many circumstances. Indeed, simulation studies suggest that such perpendicular fluctuations can arise

[a)]Electronic mail: sean@math.ucl.ac.uk
[b)]Mailing address: Code 692 NASA Goddard Space Flight Center, Greenbelt, Maryland 20771.

in multi-dimensional systems as a response to background noise. For example, $2\frac{1}{2}$D simulations of the nonlinear stage of parametric instabilities support the resonant triad description, since turbulence with large $k_\perp$ is generated following the nonlinear saturation of the lowest-order one-dimensional parametric processes.[25]

Thus, there is substantial evidence for the commonplace development of spectral anisotropy in turbulent MHD flows threaded by a large-scale magnetic field—the energy of which is at least comparable to the energy associated with the turbulence ($b/B_0 \lesssim 2$). However, a model describing the level of anisotropy as a function of plasma parameters has so far been lacking.

Here we present a simple model for the scaling of the anisotropy as a function of the fluctuating magnetic field over the total magnetic field. Our approach requires quantitative descriptions of the anisotropy and the age of the turbulence. Suitable definitions are given in the next section, prior to the model's presentation. Comparisons of the model's predictions with results from numerical simulations of incompressible and compressible MHD follow, with a discussion section closing the paper.

II. THEORY AND MODEL(S)

We denote the fluctuating (zero-mean) velocity and magnetic fields by $\mathbf{v}$ and $\mathbf{b}$, respectively, with both quantities being functions of space $\mathbf{x}$ and time t. The total magnetic field is $\mathbf{B}=B_0\hat{\mathbf{z}}+\mathbf{b}$, where B_0 is a uniform constant. Angle brackets indicate spatial averaging, so that $b=\sqrt{\langle \mathbf{b}\cdot\mathbf{b}\rangle}$ is the rms value of the fluctuating magnetic field, etc. The Fourier transform of $\mathbf{v}(\mathbf{x})$ is denoted by $\mathbf{v}(\mathbf{k})$, and similarly for the other fields. The units and initial conditions (ICs) are such that when $B_0=1$, the mean field, $\mathbf{v}$, and $\mathbf{b}$ each have the same (initial) energy.

As a quantitative measure of spectral anisotropy, it is convenient to use the *anisotropy angles*, $\theta(t)$.[11,17] For example, for the velocity field, $\theta_v(t)$, is defined by

$$\tan^2\theta_v=\frac{\Sigma k_\perp^2|\mathbf{v}(\mathbf{k})|^2}{\Sigma k_\parallel^2|\mathbf{v}(\mathbf{k})|^2}=\frac{\langle k_\perp^2\rangle_v}{\langle k_\parallel^2\rangle_v}, \tag{1}$$

where $\mathbf{k}$ is the Fourier wavevector with components $k_\parallel$ and $\mathbf{k}_\perp$ parallel and perpendicular to $\mathbf{B}_0$, and the summations extend over all retained wavevectors. The v subscript on the angle brackets indicates the weighting field. Physically $\tan\theta_v$ is a ratio of (energy-weighted) rms wavenumbers computed perpendicular and parallel to the mean magnetic field. Three special cases are relevant: isotropic fluctuations have $\theta\approx 54°$, purely parallel (slab) fluctuations have $\theta=0°$, and fully perpendicular (2D) fluctuations have $\theta=90°$. Anisotropy angles for other fields are defined in direct analogy to (1). We shall make considerable use of θ_ω, where $\boldsymbol{\omega}=\nabla\times\mathbf{v}$ is the vorticity. As discussed elsewhere, the anisotropy angles tend to increase with time—indicating evolution towards quasi-2D flows—provided the energy associated with $\mathbf{B}_0$ is at least comparable to the energy of the turbulent fluctuations.[11,14,17,18,20]

Since the anisotropy angles are functions of time, we must ensure that the different turbulent flows are compared at the same relative state of evolution, i.e., at the same turbulence age. If $E(t)$ is the total fluctuating energy of the flow (kinetic plus magnetic), then the instantaneous energy decay timescale $\tau(E)$ is defined by

$$\frac{dE}{dt}=-\frac{E}{\tau}. \tag{2}$$

This timescale can be used to define a dimensionless time t' interpreted as the age of the turbulence in characteristic energy decay times. Let dt be an unnormalized time increment, and $dt'=dt/\tau$ the corresponding normalized time increment. Integrating this last equation we obtain

$$t'(t)=-\int_0^t \frac{1}{E}\frac{dE}{dt}\,dt=\log\left[\frac{E(0)}{E(t)}\right]. \tag{3}$$

Thus, turbulent systems are of the same intrinsic (or turbulence) age when the same fraction of their initial energy has been dissipated.[26] Below, we will find it convenient to compare simulations at t_{60}, defined as the time when 60% of the initial energy remains.

We are now ready to consider the anisotropy scaling model. Previous results[11,17,18,20] have shown that for decaying MHD turbulence, greater dc magnetic field strengths lead to increasing levels of dynamically appearing anisotropy. This may be understood straightforwardly, if not rigorously, through the following over-simplified argument. For incompressible MHD each Fourier mode has two relevant timescales: the Alfvén timescale, $\tau_A=1/|\mathbf{k}\cdot\mathbf{B}_0|$, associated with wave-like effects, and the nonlinear timescale, $\tau_{NL}=1/(kv_k)\approx 1/(kb_k)$, associated with effects like advection and magnetic tension, where b_k^2 is approximately the magnetic energy associated with modes of wavenumber k.[27] The modes can thus be divided into two distinct kinds, those with $\tau_{NL}\leqslant\tau_A$, and those where the inequality is reversed.[6,13]

In RMHD efficient energy transfer occurs for modes with $\tau_{NL}\lesssim\tau_A$.[6] This relation is most restrictive when τ_{NL} is the global eddy-turnover time $1/(k_c b)$, since the nonlinear time typically decreases with scale (k_c is the wavenumber corresponding to the correlation length of the turbulence, λ_c). Thus,

$$k_\parallel \lesssim k_c\frac{b}{B_0}. \tag{4}$$

This gives an estimate for the maximum parallel wavenumber excited dynamically by RMHD activity, denoted here by $k_\parallel^{(R)}$. More specifically, in the derivation given by Montgomery,[6] it is clear that the RMHD description pertains to those excitations for which the Alfvén wave period is not shorter than the timescales associated with "slow," or nonlinear, processes. For small expansion parameter ϵ and strong magnetic field $B_0=O(\epsilon^{-1})$, the Montgomery derivation restricts RMHD to slow variations along B_0, i.e., $k_\parallel\sim\partial/\partial z=O(\epsilon)$.

Now, by definition, $\cos^2\theta_v=\langle k_\parallel^2\rangle_v/\langle k^2\rangle_v$, and $\langle k^2\rangle_v=\Omega/E\propto k_T^2$, where Ω is the enstrophy (mean-square vorticity) and k_T the Taylor microscale wavenumber.[28,29] So writing $\langle k_\parallel^2\rangle_v=\alpha[k_\parallel^{(R)}]^2$, for some constant α, we obtain

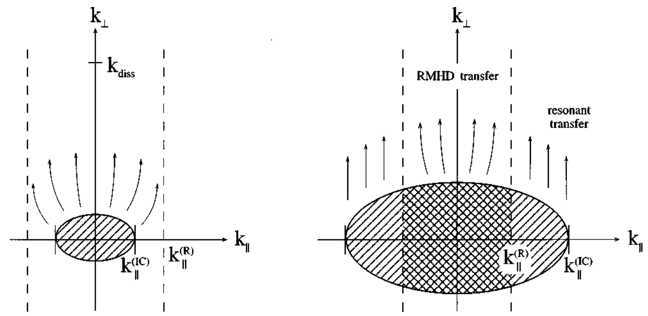

FIG. 1. Cartoon sketches of the physics behind the scaling relations, Eqs. (5) and (6), and the effects on the spectral anisotropy of initial data width (in Fourier space) and Reynolds number. Arrows indicate the direction of spectral transfer.

$$\cos^2\ \theta_v \simeq \alpha\left(\frac{k_c}{k_T}\right)^2\left(\frac{b}{B_0}\right)^2 \simeq \alpha\left(\frac{\lambda_T}{\lambda_c}\right)^2\left(\frac{b}{B}\right)^2. \tag{5}$$

In the final equation we have replaced B_0 with $B = \sqrt{B_0^2+b^2}$, a measure of the total field strength. This has the advantage of keeping the RHS bounded (and thus $\cos\ \theta_\omega \leqslant 1$) as $B_0 \to 0$ (where RMHD ceases to be valid), but making no significant difference when B_0 is large, as has already been assumed by using RMHD arguments. The ramifications of this patching are discussed later.

While a simple proportionality between $\cos^2\ \theta_v$ and $(b/B)^2$ is appealing, the neglect of various important effects in the above argument suggests that a linear relation may be more accurate. In particular, modes with $\tau_{NL} > \tau_A$ are likely to play a role.[13] We have been implicitly assuming that there is negligible energy in Fourier modes with $k_\parallel > k_\parallel^{(R)}$, and that there is no energy transfer to such modes, i.e., that *all* modes are ''Strauss-like'' or RMHD in character. This need not be the case. For example, the initial conditions may contain fluctuations which have their $k_\parallel$s outside the RMHD bandwidth. It follows that the width of the initial conditions in k-space has an impact on the (equilibrium) anisotropy level. Specifically, if $k_\parallel^{(IC)}$ is the maximum parallel wavenumber excited in the initial data then there are two cases to consider (cf. Ref. 13).

Case (1): $k_\parallel^{(IC)} \leqslant k_\parallel^{(R)}$. This is essentially the situation considered above. Initially spectral transfer occurs in all directions, but once energy reaches the RMHD ''wall'' at $k_\parallel^{(R)}$, efficient transfer of excitation to higher $k_\parallel$ is stymied [Figure 1(a)]. However, the perpendicular cascade continues until the dissipation scale k_{diss} is reached.[30] At equilibrium, then, we anticipate that $\cos\ \theta_v \approx k_\parallel^{(R)}/k_{diss}$.

Case (2): $k_\parallel^{(IC)} > k_\parallel^{(R)}$. Here there are two distinct dynamical regimes. Modes with parallel wavenumbers less than the limiting RMHD value behave as in Case (1). The remaining modes, however, are subject to a resonant interaction, where two of them may be catalyzed by a $k_\parallel = 0$ mode.[11] This process causes energy to be transferred to modes with higher $k_\perp$, but *fixed* $k_\parallel$. See Figure 1(b) and the discussion of resonant triad interactions in the introduction. Clearly, both the energy in the strict-2D component of the turbulence ($k_\parallel = 0$) and the energy in the non-RMHD (aka resonant or non-Strauss) modes is important in determining the efficacy of the resonant process. Under the assumption that the perpendicular transfer rates are roughly the same in each wavenumber regime, we may estimate the equilibrium anisotropy from $\cos\ \theta_v \approx k_\parallel^{(IC)}/k_{\rm diss}$.[31]

This discussion indicates how the scaling relation (5) can be improved upon. Let the kinetic energy be $E = E_R + E_N$, where the subscripts R and N indicate contributions from RMHD and non-RMHD modes, respectively. Breaking the sum in the definition of $\langle k_\parallel^2 \rangle_v$ into the same types of contributions, and writing $\Sigma_N k_\parallel^2 |\mathbf{v}(\mathbf{k})|^2 = 2\beta E_N [k_\parallel^{(IC)}]^2$, for some constant β, we obtain

$$\cos^2\ \theta_v \approx \frac{\alpha E_R}{E}\left(\frac{k_c}{k_T}\right)^2\left(\frac{b}{B}\right)^2 + \frac{\beta E_N}{E}\left(\frac{k_\parallel^{(IC)}}{k_T}\right)^2, \tag{6}$$

$$= m\left(\frac{b}{B}\right)^2 + c, \tag{7}$$

where we have again substituted B for B_0 to ensure sensible behavior of the model as $B_0 \to 0$. Naturally, the entire argument may be carried through for fields other than $\mathbf{v}$. For example, in the case of the vorticity $\boldsymbol{\omega}$ we obtain an equation structurally identical to (6), but with the kinetic energies replaced by the appropriate enstrophy contributions, and the correlation scale and Taylor microscale replaced by the analogous quantities based on $\boldsymbol{\omega}$, e.g., $k_T \to P/\Omega$, with P the palinstrophy. For reasons discussed in the following sections, we prefer to present our results in terms of scalings involving θ_ω.

Notice in Eq. (6) that $\cos\ \theta_v$ is approximately linear in b/B when $E_R/E \to 1$ (and $E_N/E \to 0$) for fixed values of the other constants. In the opposite limit, when most of the energy lies outside the RMHD regime, $\cos\ \theta_v \to$const. Apart from the (B_0 dependent) partitioning between R and N modes, this simplified treatment of the anisotropy depends on other constants (α, β, k_c, k_T) that characterize the spectral shapes within the R and N regions. In the present paper our emphasis is on the qualitative nature and physical origins of the anisotropy and its scaling, and we therefore defer to future work attempts to accurately predict these constants. It is also worth emphasizing that the model is essentially only valid for small b/B_0. The $B_0 \to 0$ limit is crudely accounted for by replacing B_0 with B in the slope m [see Eq. (5)], and is thus unlikely to accurately represent the true physics for the full range of b/B (see Sec. IV). Nonetheless, as shown in the next section, the agreement between simulation data and scaling relations like Eq. (6) is encouragingly good—particularly for intermediate values of b/B—and suggests that the model provides a useful description of the underlying physics.

III. SIMULATION RESULTS

A crucial assumption in the above models is that parallel spectral transfer is ''frozen out.'' Weak turbulence models for anisotropy generation[11–13] indicate that at leading-order this is correct for non-RMHD modes. While higher-order effects almost certainly involve some parallel transfer, for the present purposes we have neglected this.

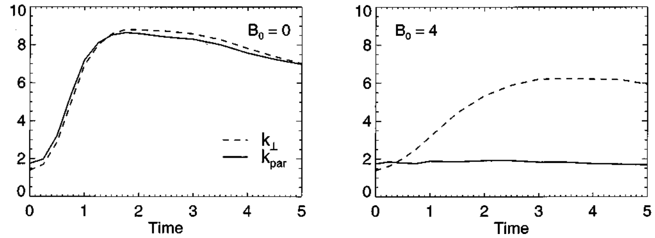

FIG. 2. The variation of mean parallel and perpendicular wavenumbers (vorticity weighted) with time for various B_0. Data are from run set B.

Numerical support for the suppression of parallel transfer is also available. Figure 2 displays time histories of the square roots of $\langle k_\parallel^2 \rangle_\omega$ and $\langle k_\perp^2 \rangle_\omega /2$ for two runs with the same initial conditions, apart from their values of B_0 (the factor of a half in $\langle k_\perp^2 \rangle$ accounts for the two degrees of freedom present in this quantity). It is evident that as B_0 increases, spectral transfer in the parallel direction is increasingly suppressed. Indeed, for $B_0 \gtrsim 2$ there is essentially no parallel transfer. The same type of behavior is seen for all run sets listed in Table I. Note that there is also a (smaller) reduction in $\langle k_\perp^2 \rangle_\omega$ as B_0 is increased. Since the initial conditions are isotropic, this is expected as much of the initial energy is then subject to the Alfvén decorrelation effect,[32,33] and indeed continues to be until the anisotropy has established itself. Put differently, prior to formation of the (strongly) anisotropic state many of the excited modes are *not* quasi-perpendicular and so their spectral transfer is strongly influenced by B_0.

Figure 3 shows a plot of $\cos^2 \theta_\omega$ as a function of $(b/B)^2$. The data points are taken from distinct spectral-method simulations of the standard (and unforced) 3D MHD equations. Each simulation has a different value of B_0 but the same (broadband) *isotropic* initial conditions; θ_ω is always evaluated at t_{60}, the wall-time at which 60% of the initial energy remains. Relevant run parameters are listed in Table I with further particulars given elsewhere;[17,18] R_e and R_m are the kinetic and magnetic Reynolds numbers. Most of the variation in b/B is due to the different values of B_0 used in each run. Least-squares straight-line fits to the data indicate that the scaling relation,

TABLE I. Simulation parameters for the runs. Each row is associated with a set of runs having the same initial **v** and **b**. Different rows have different ICs, except that the final three rows all employ the same IC (with uniform ρ). All initial conditions are isotropic and have $\nabla \cdot \mathbf{v} = 0$. Initial values for the sonic Mach number M_s and the (large-scale) kinetic and magnetic Reynolds numbers R_e, R_m are listed. The plasma β is given by $\beta_p = (B_0 M_s)^{-2}$.

Runs	B_0	M_s	$R_e = R_m$	k's initially excited
A	0,0.1,1,1.5,2,3,8	0	200	1–3
B	8,4,0	0	200	1–3
C	0.4,0.6,0.8,1,1.2,1.5,2,4,8	0	200	1–8
D	0,0.8,1,1.2,1.5,2,4,8	0	250	1–8
s00,s01,s07,s08	0,1,4,2	0.15	250	1–8
s02–s04	1,2,4	0.5	250	1–8

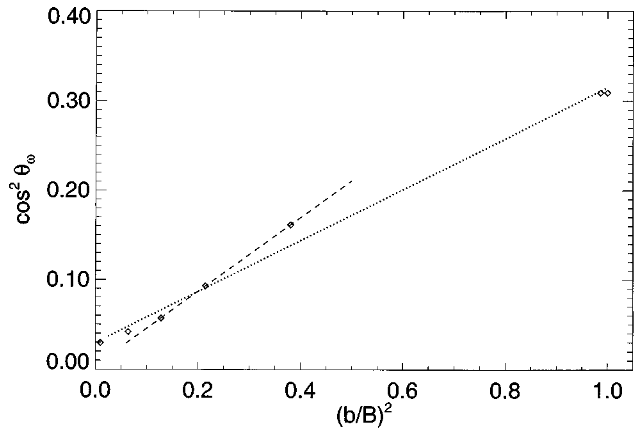

FIG. 3. Scaling of spectral anisotropy with $(b/B)^2$. Recall $B = \sqrt{B_0^2 + b^2}$. Data points are from run set A (Table I), each of which has a different value of B_0 but otherwise identical initial conditions. Two least-squares best-fits are shown: one to all the data points (dotted), and another to data points with intermediate values of b/B (dashed).

$$\cos^2 \theta_\omega = m' \left(\frac{b}{B} \right)^2 + c', \tag{8}$$

is a good approximation to the true relation in two ways. First, it is an excellent approximation over a restricted range of values of b/B, namely those not too close to 0 or 1 (dashed line). Second, it is also a useful, but clearly cruder, approximation for all values of b/B (dotted line). Hereafter, we focus mainly on the intermediate b/B case, since the physics of our model is most relevant here. As shown in the previous section and discussed further below, the slope m' and the y-intercept c' are functions of the Reynolds number(s), the initial thickness of the fluctuations in the $k_\parallel$ direction, and the partitioning of excitation between R and N type modes.

The particular choice of t_{60} is governed by several factors. First, it corresponds to roughly two large-scale eddy-turnover times, so that the turbulence has had adequate time to establish its nonlinear correlations (see, for example, Fig. 3 in Ref. 17). Second, the turbulent dynamics is still significantly nonlinear at this point, so that the anisotropy generation process is active. At later times the nonlinear dynamics is weaker because of the modest computational Reynolds numbers available. We note in passing that for the simulations discussed here, the wall-times (in units of initial large-scale eddy-turnover times) corresponding to t_{60} lie between roughly 1 and 4. Discussion on the appropriateness of θ_ω as the primary diagnostic is presented in the final section.

The argument leading to Eqs. (5) and (6) can be modified in various ways to motivate several other scalings [e.g., $\cos \theta_\omega \sim (b+B_0)/\sqrt{(b+B_0)^2 + b^2}$]. This is accomplished by employing different models for the characteristic timescales. For example, replacing k_c in τ_{NL} with $k_{c,\perp}$ may be appropriate since $k_\parallel$ is probably largely irrelevant to the quasi-2D nonlinear dynamics. However, in terms of both visual appearance and χ^2 tests, Eq. (8) has almost always provided the best fits to the simulation data. For consistency all the figures presented use scalings based on Eq. (8).

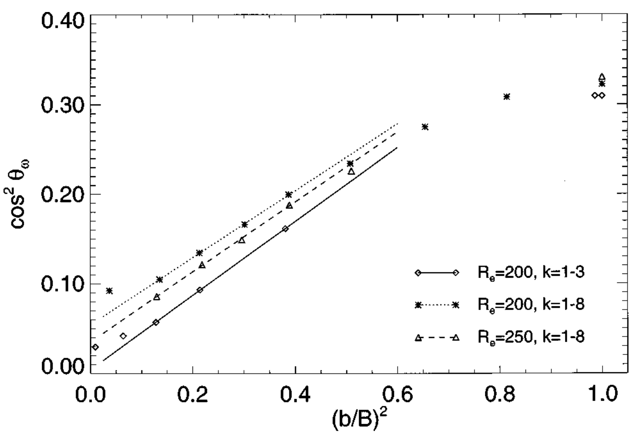

FIG. 4. Scaling relations for (sets of) runs with different Reynolds number and different width of initial conditions.

A. Dependence on turbulence parameters

The physics associated with Eq. (6) enables two qualitative, numerically testable predictions to be made. First, since in the perpendicular direction the largest dynamically active wavenumber is determined by the dissipation scale, or equivalently by the Reynolds numbers,[30,34] increasing the Reynolds numbers should result in higher average $k_\perp$ excitations for both R and N modes. Consequently, higher R_e should result in greater spectral anisotropy, as manifested here by larger values of θ_ω.

The second prediction concerns parallel transfer. Assume that the excitations fill the R-mode channel and extend into the N-mode region so that Case (2) above pertains. If B_0 is strong enough to freeze out parallel transfer (cf. Fig. 2), then the mean parallel wavenumber becomes sensitive to $k_\parallel^{(IC)}$, which for the present purposes is assumed to be determined by the ICs. It follows that runs with ''thinner'' (parallel) ICs should be more anisotropic than those with ''thicker'' ICs (e.g., see Table I, run sets A and C), provided other parameters permit approximately equal perpendicular transfer of R- and N-mode energies.

To examine these expectations we again plot $\cos^2 \theta_\omega$ vs b^2/B^2 (Fig. 4), but this time including data from runs with different Reynolds numbers and initial conditions. In all cases the least-squares best-fits are performed only for data points with $0.15 < b/B < 0.45$. The diamonds and solid curve are for the same data as in Figure 3: thin ICs, $R_e = 200$. Compared to this the dotted trace, which is the best-fit to data with thicker ICs but the same R_e, has a shallower slope and a larger y-intercept. This corresponds to reduced anisotropy, in accord with the second prediction made above. Lying between these two curves is the best-fit line for simulations with thick ICs but higher $R_e = 250$ (dashed). The associated anisotropy is increased relative to the lower R_e, same IC-thickness data, but reduced relative to the lower R_e, thinner IC-thickness data. This is consistent with both of the predictions. The fact that the anisotropy varies in accordance with the above expectations, at least for the moderate variations of parameters that we have attempted, lends credence to the physical picture underlying the model.

Note that according to Eq. (6) increased R_e—and thus increased k_T, at fixed $k_\parallel^{(IC)}$ should produce lower values for both m and c, if all other parameters remain unchanged. The Figure 4 data indicate that only c decreases, thereby implicating changes in factors like the R-N energy partitioning and the correlation lengths. It should also be borne in mind that the simulation data are for relatively low R_e turbulence, whereas the model assumes high values for the Reynolds numbers.

We have also performed a limited number of other runs with the same parameters as run set A, but which use a different realization of the initial fluctuations, i.e., the Fourier phases and (small) cross helicity are different. Over appropriate ranges of b/B the best-fit lines for these two sets of runs have slopes which differ by less than 3%. Such near equivalence for different realizations of the turbulence indicates that the governing parameters for the scaling relation coefficients are indeed likely to be independent of the IC details.

B. Compressible results

Various compressible (polytropic) simulations,[18] with initial sonic Mach numbers of $M_s = 0.15$ and 0.5, have also been performed (Table I). Our definition of the plasma beta $[\beta_p = c_s^2/V_A^2 \equiv 1/(B_0 M_s)^2]$ is based on B_0 rather than the total magnetic field $\mathbf{B}_0 + \mathbf{b}$, since we are primarily interested in cases with $B_0 \gtrsim 1$. Comparisons with alternative definitions of β_p are readily accomplished by noting that for all runs listed in Table I, b^2 is initially unity. Further details on these runs are given elsewhere.[18]

Even though the anisotropy scaling model presented above takes no account of compressive effects, knowledge of the character of magnetoacoustic fluctuations allows qualitative predictions to be made regarding changes in anisotropy when the system is (weakly) compressible. The dispersion relations of linear wave theory demonstrate that fast magnetoacoustic waves propagate approximately isotropically, and so will tend to reduce the net anisotropy, relative to an otherwise equivalent incompressible flow. Slow modes propagate more anisotropically and thus their influence is harder to assess at this level (for both modes there is also a dependence on β_p). So to the extent that linear wave theory is valid in nonlinear simulations,[25,35,36] one might expect the presence of fast modes, and possibly also slow modes, to be associated with reduced anisotropy angles. In fact, simulations[18] of low Mach number MHD turbulence show that the longitudinal (compressional) velocity fluctuations display a strong tendency towards isotropy over the range of β_p investigated $(\frac{1}{4} \lesssim \beta_p \lesssim 44)$, even when the solenoidal component of $\mathbf{v}$ is highly anisotropic. Nonetheless, the same simulations reveal that for isotropic and solenoidal initial conditions, (low M_s) compressive activity typically only slightly reduces the spectral anisotropy of $\mathbf{v}$ and $\mathbf{b}$.

Moreover, several lines of research indicate that often much of the behavior occurring in (sub-sonic) compressible systems is controlled by incompressible dynamics. Theoretical developments show that turbulence can often be treated within the framework of nearly incompressible (NI) theory,[7,9,37] wherein the leading-order fluctuations are in-

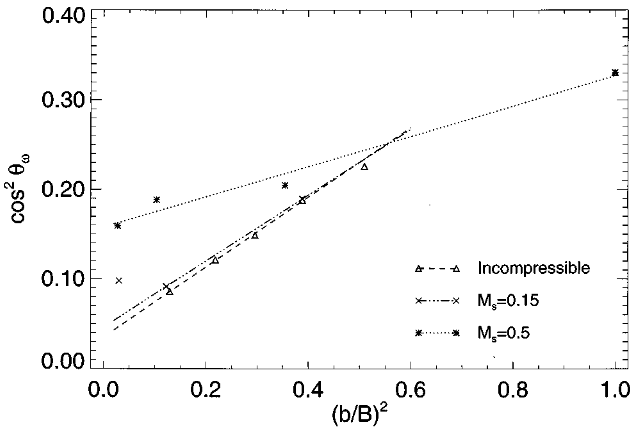

FIG. 5. The same as for Figure 4, but with compressible data also included. All data points are for $R_e=250$ runs with ''thick'' ($k=1-8$) ICs. The least-squares best-fits are for ''intermediate'' values of b/B, except for the $M_s=0.5$ case where all the data points are used.

compressible with magnetoacoustic fluctuations playing a secondary role—provided the nonsolenoidal component of the initial velocity fluctuations is small. Simulation studies also provide evidence that, at least as far as spectral anisotropy is concerned, NI theory is valid for a wider range of initial conditions than have so far been rigorously justified.[18] We therefore expect the strongly anisotropic incompressible component to be dominant, with small corrections due to the existence of a halo of isotropic compressive fluctuations.

Related work on anisotropies in the Hall MHD system[38] shows that significant fast and slow mode activity only occurs if the wavevectors lie within 45° of $\mathbf{B}_0$. While fast modes also appear at larger wavevector angles, they only do so in the dissipation range and are thus not relevant to the present discussion. The oblique, weakly dissipative region of the Hall MHD spectrum ($|\hat{\mathbf{k}}\cdot\hat{\mathbf{B}}_0|>45°$ and $k_\perp<k_{\rm diss}$) is marked by strong density–magnetic energy anti-correlations[39] and essentially zero correlation between the density and longitudinal velocity. This is consistent with NI theory predictions. The fluctuation energies are also largest in this region of wavevector space, indicating that the (quasi-)perpendicular Fourier modes are also energetically dominant for Hall MHD.

Thus, for various reasons, compressible runs—although still exhibiting anisotropy of the quasi-2D type—are expected to be somewhat less anisotropic relative to analogous incompressible runs. In terms of the scaling relation (8) this implies shallower slopes and larger y-intercepts. Figure 5 shows relevant data points for various compressible and incompressible runs, all with $R_e=R_m=250$. As a baseline we use the thick-IC incompressible data of Figure 4 (run set D). Almost overlying the best-fit curve to the intermediate b/B data is that for the $M_s=0.15$ data (dash–dot). This correspondence strongly suggests that these runs are NI in character,[7,9,37] although we have not checked this in detail. The third curve (dotted) is for the higher Mach number ($M_s=0.5$, all points) runs, and is much less anisotropic. Higher M_s is likely to be associated with greater magnetoacoustic activity, which, as noted, tends to decrease the anisotropy relative to incompressible situations, so that the results are in accord with qualitative expectations.[18,36]

IV. DISCUSSION

We have shown, using theory and numerical simulations, that to a good approximation $\cos^2\theta_\omega$ can be modeled as a linear function of $(b/B_0)^2$. It is evident that the scaling relation can only be valid for intermediate values of b/B_0, and we have presented physically motivated arguments for departures from this scaling for both small and large B_0. We have also discussed sensitivity of the anisotropy to variations of Mach number, Reynolds numbers, and initial condition bandwidth, and numerically verified these expectations.

Several issues regarding the scaling in Eq. (6) require discussion. For example, for large B_0 Eq. (6) suggests that the anisotropy saturates, provided of course that other parameters do not contain a hidden dependence on B_0 (see below). The saturation level should depend on the distribution of energy between RMHD and non-RMHD modes, and in our simple model presupposes a ''freezing out'' of parallel spectral transfer. Two cases arise, involving the extent of excitations in the perpendicular and parallel directions. The former is always limited by the dissipation wavenumber, while the latter is limited either by the wavenumber beyond which wave propagation effects induce freeze-out of parallel transfer, or by the wavenumber describing the parallel bandwidth of the ICs. Our model estimates these effects in an extremely simplified way. However, we expect that the physics of the above arguments is somewhat more robust than the precise values of the coefficients estimated in relations like Eq. (7). More quantitative evaluation of these predictions is deferred to future work.

At the other extreme, $B_0\to 0$, the ratio b/B_0 becomes unbounded and $\cos\theta\leqslant 1$ cannot be satisfied (physically, as the influence of B_0 decreases, wave effects become progressively weaker and energy transfer increasingly isotropic). As we have shown the model can be patched up by replacing B_0 with B in the above ratio. The correction is small when B_0 is not small, but restricts the ratio to values less than unity as $B_0\to 0$, allowing the isotropic value for $\cos\theta_\omega$ to be recovered, if one wishes to employ a linear fit over the entire range of values of b/B.

Unfortunately this introduces another problem. Consider increasing the Reynolds number, and thus also k_T. Equation (6) then indicates that m and c both decrease, predicting greater anisotropy at fixed b/B. The latter effect is consistent with both the physics and the simulation data. However, if we also insist that the linear relation goes through the isotropic point associated with $b/B\to 1$ and $\cos^2\theta\to\frac{1}{3}$, then it is impossible to pivot the straight line about this point and simultaneously decrease both the slope and the y-intercept. Since our arguments are predicated on the presence of a significant B_0, and essentially only crudely patched to give sensible behavior as $B_0\to 0$, it is not surprising that this limit is the source of the problem.

Indeed, Eq. (5) has the correct physics built-in, with m decreasing as k_T increases, yielding stronger anisotropy for given b/B_0. In this case, however, the linear scaling pivots about the origin, with the $B_0 \rightarrow 0$ limit simply being outside the model's scope. Despite these limitations, the linear scalings fit the simulation data encouragingly well, and the model appears to be a good and useful approximation as it stands.

Nonetheless, there are several possible remedies to the above small B_0 defect. Perhaps the simplest is to let the slope m depend on $\epsilon = (b/B)^2$. Assuming that as $\epsilon \rightarrow 0$ the RMHD physics is correct we require that $m(\epsilon)$ approach the value of m defined by Eqs. (6) and (7). At the other limit, $\epsilon \rightarrow 1$, recovery of isotropy mandates that $m \rightarrow \frac{1}{3} - c$. Interpolating linearly between these extremes gives

$$\cos^2 \theta = \left[\frac{1}{3} - (m+c)\right]\left(\frac{b}{B}\right)^4 + m\left(\frac{b}{B}\right)^2 + c. \tag{9}$$

Clearly, there are many other models which can be constructed to bridge between the small ϵ RMHD regime and the $\epsilon \approx 1$ isotropic regime.

The choice of θ_ω as our primary diagnostic, rather than some other anisotropy angle, warrants discussion. Using the angles for the velocity, magnetic field, or electric current makes no essential difference to the quality of the scaling law fits, such as Eq. (8). The equivalence of **v**-like and **b**-like angles can be understood in terms of the Alfvén effect, wherein energy is approximately equipartitioned between kinetic and magnetic modes.[41] More importantly, however, previous work[11,17] has shown that, compared to larger scales, smaller scales are more anisotropic and achieve a given level of anisotropy sooner. This is usually explained by noting that the characteristic timescale for turbulent fluctuations decreases with length-scale, and so smaller scales have had relatively longer to try and achieve local equilibrium. Thus, for the modest Reynolds number simulations which are currently feasible, the smaller-scale eddies are probably more representative of true (high R_e) inertial range dynamics.

Unfortunately, there is also a disadvantage to employing θ_ω. The simulations discussed here are only borderline resolved, in the sense that the dissipation scale is comparable to the gridscale, rather than significantly greater than it. As discussed elsewhere[17] this is associated with underestimation of the small-scale anisotropy angles (compared to otherwise identical runs with higher resolution). However, the effect is small for the runs considered here and the values obtained can be considered as lower bounds to the true values.

A particular issue that merits further discussion is the nature of the large B_0 limit, and its possible dynamical implications. Let us take as our starting point in this parameter regime the perspective that (a) parallel spectral transfer is frozen out, and (b) (incompressible) resonant modes engage in spectral transfer only through interaction with a quasi-2D mode (low frequency, RMHD mode). (Note that in leading-order perturbation theory the resonant interaction is mediated by a strictly 2D mode that has *exactly* zero Alfvén frequency.) The second assumption is physically consistent with arguments presented previously.[11] On this basis one can readily write an estimate for the separate decay of energy of the R modes, and the N modes that interact only via these resonances. A simple theory of the Taylor–Karman type[33,40] is

$$\frac{du_R^2}{dt} = -\frac{u_R^3}{\lambda_R}, \quad \frac{du_N^2}{dt} = -\frac{u_N^2 u_R}{\lambda_N}, \tag{10}$$

where λ_N and λ_R are lengthscales associated with the energy containing eddies of the N and R types, respectively.

In this approximation the decay rate for the N modes depends on the energy levels in both types of modes, whereas R-mode decay depends only on R-mode energy. Note that in writing these equations we in effect treat the resonance width as of order $k_\parallel^{(R)}$, the parallel bandwidth of the RMHD regime. Because both kinds of turbulence are driven essentially only by R modes, it is clear that the partitioning of energy between R and N categories is important for understanding the strong B_0 limit. In particular, scaling of spectral transfer with B_0 directly influences anisotropy in this limit. For a fixed distribution of energy $E(k_\parallel) = \int d\mathbf{k}_\perp E(\mathbf{k})$, the energy u_R^2 in RMHD modes can be estimated in two entirely different ways yielding distinct conclusions.

First, consider the case appropriate to an infinite spatial domain for which $E(k_\parallel)$ is a continuously-varying finite function of $k_\parallel$ near $k_\parallel = 0$. For this case

$$u_R^2 = 2\int_0^{k_\parallel^{(R)}} dk_\parallel E(k_\parallel), \tag{11}$$

implying that $u_R^2 \sim b/B_0$, provided $E(k_\parallel = 0)$ is nonzero. Consequently, the effective eddy-turnover time $\tau_N = \lambda_N/u_R \sim \sqrt{B_0} \rightarrow \infty$ as $B_0 \rightarrow \infty$. Similarly $\tau_R = \lambda_R/u_R \sim \sqrt{B_0}$ and all turbulence is quenched in this limit. The implications for anisotropy are interesting. The extent of the spectra in the perpendicular direction in both the N and R regions is typically limited by the dissipation wavenumber k_{diss}, which is an increasing function of the spectral transfer rate. In the above limit perpendicular spectral transfer rates become vanishingly small and therefore k_{diss} is expected to decrease, and thus anisotropy would also *decrease*.

The second case of interest in the context of the $B_0 \rightarrow \infty$ limit is that of a domain of finite extent in the parallel direction. This can be modeled by a box with a large periodicity length L and associated discrete $k_\parallel$'s with spacing $1/L$. In contrast to the first case, here as $B_0 \rightarrow \infty$ we do not conclude that $u_R^2 \rightarrow 0$. In fact after B_0 becomes so large that $k_\parallel^{(R)} < 1/L$, the partitioning between u_R and u_N becomes independent of B_0, and u_R is thereafter identified with the strictly zero frequency purely 2D modes in the spectrum. Under the assumption that these modes possess nonzero energy, we conclude immediately that the decay rates of both R- and N-modes remain finite as $B_0 \rightarrow \infty$. Since the spectral transfer rates in the R and N regions become insensitive to B_0, the dissipation wavenumbers also become independent of B_0, and the turbulence approaches a limiting B_0 independent nonvanishing anisotropy.

The contrast between the above two possibilities is great: On the one hand it appears that for MHD turbulence in an infinite domain, both spectral transfer and spectral anisotropy may be suppressed for extremely strong magnetic field. For a finite system, however, spectral transfer rates and spectral anisotropy remain finite and become insensitive to magnetic field strength in the strong field limit. We note in passing that the numerical experiments do not show a reversal of the trend of increasing anisotropy for stronger B_0, which is understandable since the simulations are carried out in a finite periodic box. However, there is a hint of a saturation of anisotropy at the strongest values of B_0 computed (cf. Ref. 20). On the basis of the finite box discussion above we would expect the saturation to occur after $k_\parallel^{(R)} = k_c b/B_0 < 1$, where $k_c \approx 3-4$ in simulation units. Therefore saturation might start to occur for values of $b/B_0 \lesssim \frac{1}{3}$, and indeed such a suggestion is consistent with the results shown in Figures 3–5. The same scenario—linear scaling of anisotropy followed by saturation of decay rates at large B_0—is also consistent with earlier work that examined phenomenologies for energy decay using similar computer runs.[33]

We anticipate that the simplest linear scaling model presented here [e.g., Eq. (5)] may be useful in many applications, since this case appears to be relevant to the interesting parameter regime near $b/B_0 \approx 1$. This model is most useful when nearly all of the turbulent energy resides in RMHD modes, and resonant transfer among other modes is a small part of the energy transfer budget. Refinements to this simplest scaling relation that we described here take into account an eventual transition, for larger B_0, to a situation in which more (and perhaps most) of the energy resides in non-RMHD modes. In this case a dependence on the initial distribution of energy is observed, and the model predicts saturation of anisotropy and a concomitant saturation of energy decay rates.[33] In this latter regime resonant interactions are dominant but RMHD is formally not applicable. In spite of this it remains a matter of some interest that investigations of strong B_0 anisotropies that *begin* with the RMHD equations[13,23] arrive at conclusions that are in at least partial agreement with analyses based upon the full MHD equations, such as the present one.[6,11,17,18] We expect that the refinements in description of spectral anisotropy presented here will be of wide applicability in models of MHD turbulence, particularly those employed in space physics and astrophysics.

ACKNOWLEDGMENTS

We thank Dr. Murshed Hossain, Dr. Rodney Kinney, Dr. David Montgomery, and Dr. Duane Pontius for valuable discussions, and an anonymous referee for useful criticism. This work has been supported in part by grants from the Nuffield Foundation, the Particle Physics and Astronomy Research Council, the National Science Foundation, and by National Aeronautics and Space Association through the Space Physics Theory Programs at Bartol and the Goddard Space Flight Center.

[1] D. Robinson and M. Rusbridge, Phys. Fluids **14**, 2499 (1971).
[2] S. Zweben, C. Menyuk, and R. Taylor, Phys. Rev. Lett. **42**, 1270 (1979).
[3] W. H. Matthaeus, M. L. Goldstein, and D. A. Roberts, J. Geophys. Res. **95**, 20 673 (1990).
[4] V. Carbone, F. Malara, and P. Veltri, J. Geophys. Res. **100**, 1763 (1995).
[5] H. R. Strauss, Phys. Fluids **19**, 134 (1976).
[6] D. C. Montgomery, Phys. Scr. **T2/1**, 83 (1982).
[7] G. P. Zank and W. H. Matthaeus, J. Plasma Phys. **48**, 85 (1992).
[8] Recall that the derivation (Ref. 6) of the Strauss equations explicitly *excludes* the presence of an initial $O(1)$ population of Alfvén waves. However, if they exist, simulations (Refs. 11 and 17) show that evolution proceeds in such a way as to make the Stauss equations an increasingly valid approximation.
[9] G. P. Zank and W. H. Matthaeus, Phys. Fluids A **5**, 257 (1993).
[10] D. C. Montgomery and L. Turner, Phys. Fluids **24**, 825 (1981).
[11] J. V. Shebalin, W. H. Matthaeus, and D. Montgomery, J. Plasma Phys. **29**, 525 (1983).
[12] R. Kinney and J. C. McWilliams, J. Plasma Phys. **57**, 73 (1997).
[13] R. Kinney and J. C. McWilliams, Phys. Rev. E **57**, 7111 (1998).
[14] M. Hossain, G. Vahala, and D. Montgomery, Phys. Fluids **28**, 3074 (1985).
[15] E. Weisshaar, Geophys. Astrophys. Fluid Dyn. **41**, 141 (1988).
[16] W. H. Matthaeus, L. W. Klein, S. Ghosh, and M. R. Brown, J. Geophys. Res. **96**, 5421 (1991).
[17] S. Oughton, E. R. Priest, and W. H. Matthaeus, J. Fluid Mech. **280**, 95 (1994).
[18] W. H. Matthaeus, S. Ghosh, S. Oughton, and D. A. Roberts, J. Geophys. Res. **101**, 7619 (1996).
[19] S. Oughton, J. Plasma Phys. **56**, 641 (1996).
[20] V. Carbone and P. Veltri, Geophys. Astrophys. Fluid Dyn. **52**, 153 (1990).
[21] S. Sridhar and P. Goldreich, Astrophys. J. **432**, 612 (1994).
[22] D. C. Montgomery and W. H. Matthaeus, Astrophys. J. **447**, 706 (1995).
[23] C. S. Ng and A. Bhattacharjee, Astrophys. J. **465**, 845 (1996).
[24] P. Goldreich and S. Sridhar, Astrophys. J. **485**, 680 (1997).
[25] S. Ghosh and M. L. Goldstein, J. Geophys. Res. **99**, 13 351 (1994).
[26] W. H. Matthaeus, C. W. Smith, and S. Oughton, J. Geophys. Res. **103**, 6495 (1998).
[27] Numerous simulations, including those discussed here, verify that $v_k \approx b_k$ for sufficiently large B_0. This is usually explained in terms of the Alfvén effect (Ref. 41).
[28] G. K. Batchelor, *The Theory of Homogeneous Turbulence* (Cambridge University Press, Cambridge, 1970).
[29] The fundamental definition for the Taylor microscale is as the curvature of the longitudinal velocity autocorrelation, $\lambda_T^2 = \langle v_1^2 \rangle / \langle (\partial_1 v_1)^2 \rangle$, and for isotropic turbulence this is equal to $5E/\Omega$ (Ref. 28). Since we are primarily interested in the scaling properties, and also we cannot invoke isotropy, we have elected to drop the associated numerical factors here.
[30] A. N. Kolmogorov, C. R. (Dokl.) Acad. Sci. URSS **30**, 301 (1941).
[31] Note that the two cases are analogous to the cases considered in Ref. 13, in which the discussion is couched entirely in terms of RMHD.
[32] M. Hossain, P. C. Gray, D. H. Pontius, Jr., W. H. Matthaeus, and S. Oughton, in *Proceedings of Solar Wind 8, COSPAR Colloquia Series* (Pergamon, Oxford, UK, 1996).
[33] M. Hossain, P. C. Gray, D. H. Pontius, Jr., W. H. Matthaeus, and S. Oughton, Phys. Fluids **7**, 2886 (1995).
[34] M. Lesieur, *Turbulence in Fluids* (Nijhoff, Dordrecht, The Netherlands, 1990).
[35] S. Ghosh, A. F. Viñas, and M. L. Goldstein, J. Geophys. Res. **99**, 19 289 (1994).
[36] F. Malara, L. Primavera, and P. Veltri, J. Geophys. Res. **101**, 21 597 (1996).
[37] G. P. Zank and W. H. Matthaeus, J. Geophys. Res. **97**, 17 189 (1992).
[38] S. Ghosh and M. L. Goldstein, J. Plasma Phys. **57**, 129 (1997).
[39] See also Ref. 36 but note that the ICs in their simulations are not isotropic, so that it is difficult to say whether the observed anisotropy is a consequence of the initial data, nonlinear evolution, or perhaps both factors.
[40] T. von Kármán and L. Howarth, Proc. R. Soc. London, Ser. A **164**, 192 (1938).
[41] R. H. Kraichnan, Phys. Fluids **8**, 1385 (1965).